Environ. Sci. Technol. **1994**, *28*, 1717–1726

Effect of Solution Chemistry on Clay Colloid Release from an Iron Oxide-Coated Aquifer Sand

Joseph N. Ryan[*,†] **and Philip M. Gschwend**[‡]

Department of Civil, Environmental, and Architectural Engineering, University of Colorado, Campus Box 428, Boulder, Colorado 80309, and Ralph M. Parsons Laboratory, Department of Civil and Environmental Engineering, Massachusetts Institute of Technology, 48-415, Cambridge, Massachusetts 02139

This research compared the influence of (1) dissolution of iron oxides and (2) alteration of electrostatic interactions on the mobilization of colloids in a clay- and iron oxide-coated sand obtained from an Atlantic Coastal Plain aquifer in which colloids have been found suspended only in anoxic groundwater. The sediment was flushed with solutions of varying ionic strength, pH, and reductant and surfactant concentrations, and the steady-state rates of clay colloid release and iron oxyhydroxide dissolution were measured. The clay release rates were directly related to the calculated detachment energies and unrelated to rates of iron(III) oxide dissolution, indicating that electrostatic interactions dominated the binding of colloids to grain coatings. Mobilization of colloids by iron(III) oxide dissolution through reductive dissolution was limited by high ionic strength. Flushing of the sediment by a natural groundwater with high dissolved organic carbon concentration released clay without rapidly dissolving iron oxides.

Introduction

Concern over the source of colloids in groundwater has escalated as cases of colloid-facilitated transport of low solubility contaminants have been reported (*1–4*); however, the source of colloids responsible for enhanced transport has not always been addressed in these papers. Possible mechanisms of colloid generation in groundwater include precipitation (*5*, *6*), erosion in fractures and soils (*7*, *8*), mobilizations by changes in pH and ionic strength (*9–11*), and release by the dissolution of cementing phases (*12–15*).

In our past research, we observed that clay mineral colloids were abundant in anoxic groundwaters and absent from oxic groundwaters in two Atlantic Coastal Plain aquifers consisting of iron(III) oxide-coated quartz sands (*14*). At the New Jersey Coastal Plain site, the anoxic sediments, located beneath a swamp, contained significantly lower levels of iron(III) oxides and clay-sized particles than in nearby oxic sediments (*16*). In the oxic sediments, the quartz grains were coated by colloidal kaolinite and microcrystalline iron(III) oxide, primarily goethite (α-FeOOH). We hypothesized that (1) the goethite cemented together the kaolinite and quartz and (2) beneath the swamp, the abundant organic matter in the infiltrating water caused the dissolution of the geothite; thus, the kaolinite was mobilized by "decementation".

Alternatively, the clay colloids may have mobilized as the infiltrating grounwater caused an increase in the repulsive colloidal forces described by the DLVO (*17*, *18*) theory. For example, the introduction of fresh water into briny, oil-bearing formations typically causes clay mobilization leading to formation plugging. Some researchers (*10*, *19*, *20*) have observed that the permeability decrease occurs at a "critical salt concentration" corresponding to a primary maximum in DLVO potential energy near zero ($\phi_{max} \approx 0$; ϕ_{max} identified in Figure 1); however, $\phi_{max} \approx 0$ corresponds to the absence of an energy barrier to *attachment*, not *detachment* (*21*, *22*). To relate colloid detachment to DLVO potential energy, we must consider the energy barrier that attached particles must overcome. This energy barrier is represented by the depth of the primary minimum (ϕ_{min1}) relative to ϕ_{max}.

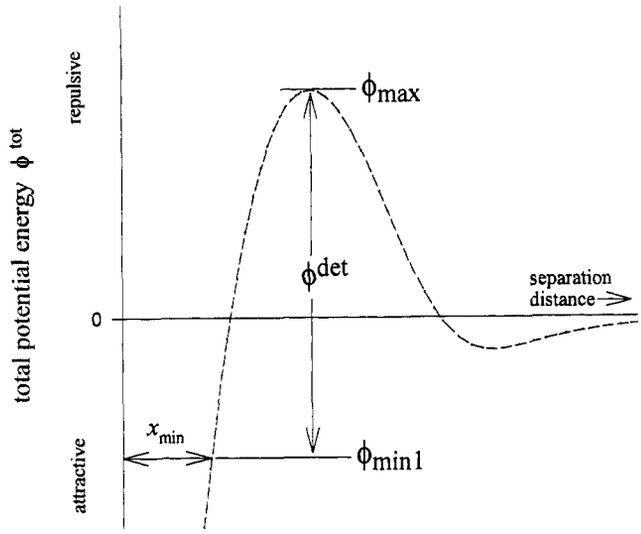

Figure 1. Total intersurface potential energy, ϕ^{tot}, between colloid and grain surfaces vs separation distance. Total potential energy is calculated as $\phi^{vdw} + \phi^{dl}$, the sum of van der Waals and electrostatic energies. A finite primary minimum (ϕ_{min1}) is designated by choosing the distance of closest approach, x_{min}. The detachment energy is the difference between the primary maximum (ϕ_{max}) and minimum energies ($\phi^{det} = -[\phi_{max} - \phi_{min1}]$).

A kinetic treatment of colloid detachment requires a ϕ_{min1} of finite depth (Figure 1), which may be estimated in two ways: (1) by assuming that a separation distance of closest approach exists (*23*) or (2) by including short-range Born potential energy in the total intersurface potential energy profile (*11*, *22*, *24–26*). With a primary minimum of finite depth, the rate-limiting step in particle detachment is the escape of particles from ϕ_{min1}; thus, the detachment rate is exponentially related to the size of the energy barrier ($\phi^{det} = -[\phi_{max} - \phi_{min1}]$), analogous to the dependence of a chemical reaction rate on the Arrhenius activation energy (*21*, *22*). Studies of detachment of colloidal oxides from porous media have shown that the colloid release rate is related to the size of the detachment energy barrier (*23*, *26*), although the relationship is not necessarily exponential.

Our goal in this research was to determine whether the forces that bind the colloids to the grains in the New Jersey

† University of Colorado; e-mail address: joeryan@spot.colorado.edu.

‡ Massachusetts Institute of Technology; e-mail address: pmgschwe@mit.edu.

0013-936X/94/0928-1717$04.50/0

Table 1. Characteristics of Natural Sediment and Groundwater Samples Collected from McDonalds Branch Watershed, Lebanon State Forest, NJ[a]

	Natural Sediment Sample (Core U.11.1)	
depth	7.3–8.8 m	
clay-sized fraction (<2 μm)	3.8 ± 0.4 wt %	sedimentation
minerals	kaolinite goethite quartz	X-ray diffraction
heavy mineral fraction (>2.89 g cm^{-3})	1.1 ± 0.1 wt %	$CHBr_3$ sedimentation
minerals	pseudorutile ilmenite rutile	X-ray diffraction
free Fe	39 ± 2 μmol g^{-1}	Ti(III) extraction (*28*)
free Al	7.2 ± 0.6 μmol g^{-1}	
total Fe	77 ± 2 μmol g^{-1}	$HF/HCl/HNO_3$ digestion
total Ti	72 ± 2 μmol g^{-1}	
organic matter	0.45 ± 0.07 wt %	loss on ignition (450 °C, 6 h)
specific surface	0.51 ± 0.10 m^2 g^{-1}	single-point N_2 BET
	Natural Groundwater in Contact with Sediment (Well QWH-4b)	
pH	4.8	combination electrode and meter
I	0.4 ± 0.1 mM	Ryan and Gschwend (*14*)
E_H	340 ± 30 mV	Pt electrode/4 M Ag–AgCl reference (relative to standard H electrode)
dissolved O_2	190 ± 10 μM	O_2 electrode and meter
Fe (<0.015 μm)	0.19 μM	GF-AAS
Fe_T	0.55 μM	GF-AAS
organic C	0.067 mM	persulfate oxidation (*29*)
colloidal clay	≤1 mg L^{-1}	light scattering; kaolinite standard curve (Coulter N4 submicrometer particle analyzer)
	Natural Groundwater Used for Flushing (Well QWH-1a)	
pH	4.2	combination electrode and meter
I	1.0 ± 0.1 mM	Ryan and Gschwend (*14*)
E_H	250 ± 25 mV	Pt electrode/4 M Ag–AgCl reference (relative to standard H electrode)
dissolved O_2	6 ± 3 μM	colorimetric test kit (Chemetrics, Inc., Calverton, VA)
Fe(II)	42 ± 0.6 μM	TPTZ complexation
Fe_T	42 ± 0.6 μM	NH_2OH reduction/TPTZ complexation
organic C	1.70 ± 0.13 mM	800 °C oxidation on Pt catalyst (*29*)
colloidal clay	0.27 ± 0.05 mg L^{-1}	light scattering; kaolinite standard curve (Hach Ratio X/R turbidity meter)

[a] For details on analytical methods, see Ryan and Gschwend (*14*, *16*).

Coastal Plain aquifer were primarily chemical (requiring decementation for colloid detachment) or physical (requiring only a change in the intersurface potential energy for detachment). To do this, we compared trends in measured colloid release rates with measured Fe release rates and predicted DLVO detachment energies (*21*, *22*). We also sought to establish an experimental means for evaluating the colloid release potential of a sediment affected by an alteration in groundwater chemistry.

Methods

Field Sampling. The sediment sample was collected during a previous study (*16*, *27*) from a saturated, oxic zone of the Late Miocene Cohansey Sand formation near McDonalds Branch in Lebanon State Forest, NJ. The sediment consists mainly of unconsolidated quartz sand coated by thin (<10 μm), anisopachous layers of kaolinite and goethite (Table 1). The coatings contain about 5 mol of kaolinite for every mole of goethite [assuming that the clay-sized fraction was composed entirely of kaolinite ($Al_2Si_2O_5[OH]_4$) and that the free Fe fraction was composed entirely of goethite]. The sample was dried at 60 °C and sifted through 1.0- and 0.25-mm sieves to improve subsample homogeneity. The 0.25–1.0-mm fraction comprised 80 wt % of the total sample. Magnetic minerals, mainly iron–titanium oxides, were removed by vibrating the sample through an acrylic trough with a thin bottom over a 0.3-T magnet.

Groundwater was collected about 50 m upstream from the sediment sampling location in November 1991, from a well screened 2 m below a swampy stream bed (McDonalds Branch). Three well volumes of water were pumped with a peristaltic pump through polytetrafluoroethylene (PTFE) and silicone tubing at a flow rate of 1 L min^{-1} into overflowed, ground glass-stoppered bottles. The samples were stored at 5 °C prior to experiments. The groundwater is acidic, anoxic, high in organic matter and Fe(II) concentrations, and relatively free of colloids (Table 1).

Reaction Column. A "column" with a short flow path (a 47-mm filter cartridge) was used to minimize reattachment of mobilized colloids. In the column, a 0.22-μm membrane filter removed particles in the incoming solutions, and a nylon screen (120 mesh) and o-ring (40 mm diameter) retained the sand. A dry, disoriented sand sample was packed into the column; as such, it did not accurately represent the original sediment. The sand formed a disk of 2.5–3.0-mm height and 40-mm diameter. The pore volume, estimated for each run by assuming a solids' density of 2.65 g cm^{-3}, varied from 1.3 to 1.9 cm^3.

The flushing solutions were titrated to proper pH with HNO_3 or NaOH after being purged with argon. Ascorbic

acid (H_2Asc) solutions were prepared in argon-purged high-purity water and wrapped in foil to curtail photooxidation. Using an HPLC pump with a pulse dampener, the solutions were pumped through a flow cell for conductivity measurement and upward through the column to ensure complete saturation. The column effluent passed through a flow cell (fashioned from a 3-mL glass pipet) in a turbidity meter (Hach Ratio X/R) and a flow cell for pH measurement. The column effluent was collected in amber glass vials flushed with argon. The entire system was connected by 1.6-mm i.d. PTFE tubing.

The experiments were performed at a flow rate 0.50 ± 0.05 mL min^{-1}, which corresponds to column residence times of 2.3–4.2 min and Darcy velocities from 1.0 to 1.6 m day^{-1}. These velocities are within the range of Cohansey sediment groundwater velocities (*30*).

Reaction Column Monitoring. The turbidity of the column effluent was measured continuously using a chart recorder, digitized, and converted to "clay" concentrations using a turbidity vs kaolinite standard curve prepared using suspensions of "colloidal kaolin powder" (EM Science, <2-μm fraction isolated by sedimentation). Turbidity (T_{NTU}) was linearly related to kaolinite suspension concentration ([K]) in our flow-through glass cell over the range of 0–10 mg L^{-1} kaolinite by

$$T_{NTU} - B = 0.623[K] + 0.004 \qquad (R^2 = 0.9986) \quad (1)$$

where B is the baseline turbidity (in NTU) for each run, determined as the turbidity of 0.22-μm filtered high-purity water ($0.05 < B < 0.09$ NTU). The actual mass concentrations of the mobilized colloids, which were checked gravimetrically by trapping colloids produced by two experiments on preweighed 0.1-μm membrane filters, were 5.1 and 11% lower than those estimated using eq 1, suggesting that the mobilized colloids and the kaolinite standards scattered light similarly within the range of error of the gravimetric analysis. To calculate the steady-state, or time-averaged, clay release rate (g min^{-1}), the total mass of clay released in a given time was divided by the flow rate. The varying baseline turbidity resulted in clay release rate detection limits of 3.7×10^{-8} to 6.9×10^{-8} g min^{-1}.

The amount of total Fe released from the column was measured spectrophotometrically ($\lambda = 595$ nm) using the Fe(II)–TPTZ complex (*31*). Hydroxylamine hydrochloride ($NH_2OH \cdot HCl$) was added prior to TPTZ to reduce dissolved iron(III) to Fe(II). The total Fe measurement had a detection limit of 35 nM and a precision of ±1.5%. The steady-state, time-averaged Fe release rate (mol min^{-1}) was calculated by dividing the steady Fe effluent concentration (mol L^{-1}) by the flow rate. The detection limit was 1.8×10^{-11} mol min^{-1}. In the natural groundwater runs, the precision was poorer because the amount of Fe released was determined as the difference between the effluent [Fe] and the natural groundwater initial [Fe].

Electrophoretic mobilities were measured at 25 °C with a Rank Brothers Mk II equipped with a cylindrical cell and a 3-mW He–Ne laser. The mobilities (U, m^2 V^{-1} s^{-1}) of 20 particles timed in both directions and at both stationary levels were converted to ζ (V) using the Smoluchowski formula (*32*), $\zeta = (U\eta)/(\epsilon\epsilon_0)$, where η is the viscosity of water, ϵ is the dielectric constant of water, and ϵ_0 is the permittivity of free space. More detailed approaches to the conversion of electrophoretic mobility to ζ were not merited owing to the complications of the irregular size and shape of the mobilized colloids. Clay concentrations in the effluent were generally too low to provide enough colloids for reliable measurement of ζ, so separate runs were made during which the columns were lightly tapped to mobilize clay in higher concentrations. We recognize the possible bias in the mobilized colloid population produced by this technique; however, this technique was necessary at low clay release rates.

Residual sand samples were collected after some runs and examined by scanning electron microscopy (SEM) and energy-dispersive X-ray spectroscopy (EDX). Suspended particles trapped on 0.1-μm membrane filters were also examined. The column residues and filtered particles were air-dried, mounted on Al stubs with colloidal graphite, and Au and Pd coated.

Experimental Procedures. The experimental conditions are summarized in Table 2. Each column was packed with dry sand and flushed first by a high I (ionic strength) solution to remove only those particles loosened during column packing. The high I flushes were followed by low I flushes, which provided baseline clay release rates against which the experimental clay release rates could be compared. The low I flushes were run until turbidity reached stable levels comparable to the background turbidity, which required at least 20 pore volumes in every run. Most of the solutions contained a dilute acetic acid/acetate (HAc/Ac^-) solution which aided in buffering pH near the ambient pH of the groundwater in the oxic sediment.

In the ΔI and duplicate ΔpH experiments, successively lower I and higher pH solutions were sequentially run through single columns. In the ΔH_2Asc experiments, ascorbic acid concentration was varied at pH 4.8 and 6.0 in separate columns for each reductant concentration. The reductant solutions were followed by low I flushes at the same pH. In the ΔpH H_2Asc experiment, successively higher pH reductant solutions were separated by intervening low I flushes at the next higher pH. In duplicate ΔRCOOH experiments, dodecanoic acid [$CH_3(CH_2)_{10}COOH$; or RCOOH] solutions were separated by low I flushes. Dodecanoic acid solutions were separated by low I flushes at the next higher pH. Unamended natural groundwater collected from the field site was also used to flush the sediment.

Calculating Detachment Energy. We estimated the detachment energy as $\phi^{det} = -[\phi_{max} - \phi_{min1}]$ using the sum of the van der Waals and double-layer potential energies as the total potential energy calculated as a function of separation distance. To define a ϕ_{min1} of finite depth, we assumed a distance of closest approach. Although the colloids were clay plates with different surface potentials on faces and edges, we decided to represent them as uniformly charged spheres because (1) the plates appeared to be randomly oriented in the grain coatings and (2) ζ could be measured only as an overall parameter.

The van der Waals potential was calculated with the Hamaker (*33*) expression for the unretarded interaction of two spheres. The double-layer potential was calculated with the Hogg *et al.* (*34*) expression for sphere–sphere interactions and constant potentials. Note that the accuracy of the Hogg *et al.* expression, a linearized solution of the Poisson–Boltzmann (PB) equation, decreases for $\psi_0 > 25$ mV and small separation distances (compared to an exact solution of the full PB equation), so our estimates

Table 2. Summary of Experimental Conditions Including Composition and Number of Pore Volumes (PV) of Solutions Run through Columns[a]

experimental variable	high I flush	low I flush	experiment	post-flush
ΔI	0.5 M $NaNO_3$; 5×10^{-4} M Ac; pH 4.8; ≥40 PV		$0.5–6 \times 10^{-5}$ M $NaNO_3$; sequential; 20 PV each	
ΔpH	0.5 M $NaNO_3$; 5×10^{-4} M Ac; pH 2.0; ≥20 PV	0.01 M $NaNO_3$; 5×10^{-4} M Ac; pH 2.0; ≥20 PV	0.01 M $NaNO_3$; 5×10^{-4} M Ac; pH 2.0–10.0; sequential; 20 PV each	
ΔH_2Asc	0.5 M $NaNO_3$; 5×10^{-4} M Ac; pH 4.8, 6.0; ≥20 PV	5×10^{-4} M Ac; pH 4.8, 6.0; ≥20 PV	1×10^{-4}–0.1 M H_2Asc; 5×10^{-4} M Ac; pH 4.8, 6.0; separate columns; >45 PV each	5×10^{-4} M Ac; pH 4.8, 6.0; following reduction; >45 PV each
ΔpH H_2Asc	0.5 M $NaNO_3$; 5×10^{-4} M Ac; pH 3.0; ≥20 PV	5×10^{-4} M Ac; pH 3.0; ≥20 PV	1×10^{-3} M H_2Asc; 5×10^{-4} M Ac; pH 3.0–7.0; sequential; 20 PV each	5×10^{-4} M Ac; next pH intervening; 10 PV each
ΔRCOOH	0.5 M $NaNO_3$; 5×10^{-4} M Ac; pH 4.8; ≥20 PV	5×10^{-4} M Ac; pH 4.8; ≥20 PV	12–160 μM RCOOH; 5×10^{-4} M Ac; pH 4.8; sequential; 20 PV each	5×10^{-4} M Ac; pH 4.8; intervening; 10 PV each
ΔpH RCOOH	0.5 M $NaNO_3$; 5×10^{-4} M Ac; pH 3.0; ≥20 PV	5×10^{-4} M Ac; pH 3.0; ≥ 20 PV	80 μM RCOOH; 5×10^{-4} M Ac; pH 3.0–8.0; sequential; 20 PV each	5×10^{-4} M Ac; next pH intervening; 10 PV each
natural groundwater	0.5 M $NaNO_3$; 5×10^{-4} M Ac; pH 4.2; ≥20 PV	5×10^{-4} M Ac; pH 4.2; ≥20 PV	unamended groundwater; pH 4.2; 40, 45, 290 PV	5×10^{-4} M Ac; pH 4.2; following groundwater; >10 PV each

[a] Acetic acid/acetate buffer shown in parentheses when included in all solutions of a series. Ascorbic acid (H_2Asc) and dodecanoic acid (RCOOH) added as acids. Post-flushes either follow separate column experiments or intervene between sequential, single-column experiments.

of detachment energy are valid only for the evaluation of trends in detachment energy.

Because flushing removed only small amounts of the clay in the sediment, we assumed that the interactions controlling detachment occurred between clay colloids in the coatings and not between colloids and grains. Based on SEM examination, we estimated the average diameters of the clay colloids as 1 μm. We used a Hamaker constant of 4×10^{-20} J and a distance of closest approach of x_{min} = 7 Å. This x_{min} is within the range determined as fitting parameters in experimental systems (4–10 Å; refs 24 and 27).

Estimating Surface Potentials from ζ Potentials. At high ionic strength and surface charge, ζ fails to provide a good estimate of ψ_0 (*18*, *32*). Because ϕ^{dl} is very sensitive to ψ_0, we sought to correct our measured ζ for the effects of high ionic strength and surface charge. To avoid defining a fixed shear plane distance required by Overbeek's (*35*) expression relating ζ and ψ_0, we derived an empirical relationship between values of ζ measured for rutile (TiO_2) and alumina (γ-Al_2O_3) by Wiese and Healy (*36*) and surface potentials calculated for these simple oxides with a surface complexation/double-layer (SCDL) model (ψ_{scdl}) following Dzombak and Morel (*37*).

Values of ψ_{scdl} for rutile and alumina or the pH and I range over which ζ was measured were calculated using parameters recorded in Ryan (*27*). The equilibrium reactions were solved with a version of MINEQL (*38*) modified to account for Gouy–Chapman double-layer interactions (*37*). For a range of ionic strengths, ζ (mV) was fit to ψ_{scdl} (mV) to arrive at the following empirical expression:

$$\psi_{scdl} = \zeta + [e^{4.7\times10^{-4}\kappa^{0.28}\zeta} - 1] \quad (2)$$

where κ is the Debye–Hückel parameter. This expression is similar in form to Overbeek's $\zeta - \psi_0$ relationship (*35*) with the exception that it does not require identification of a fixed distance to the shear plane. This empirical expression is not intended to elucidate any of the causes for the disparity between ζ and ψ_0.

Results

Morphology and Composition of Sediment and Mobilized Colloids. After the high I/low I flushes, loose coatings remained on the grain surfaces. Ascorbic acid reduction removed much of the coatings on smooth faces of the grains, while surface irregularities and intergrain contacts remained filled with coatings. The same coating distribution was observed in the natural sediments found in the path of the infiltrating organic matter (*16*).

The released colloids contained roughly equal concentrations of Al and Si (as well as <0.5–3.0 mol % of Fe) and were predominantly <2-μm diameter (*27*), similar to those found in the natural groundwater (*14*). Discrete iron(III) oxide colloids were not detected under any column conditions, although such colloids were found suspended in the natural groundwater.

The isoelectric point (pH_{iep}) of the colloids released from the column was the same as that of natural groundwater colloids (*14*), about 3.0. The values of pH_{iep} measured for pure kaolinite by microelectrophoresis range from 3.3 to 5.0 (*39*); thus, we surmise that adsorption of organic matter lowered the pH_{iep} of the clay colloids.

Sediment Flushing Experiments. The results of a high I/low I column preparation flush show that (1) the high I flush removed a large amount of clay that we assume was disrupted by column packing and (2) the low I flush removed a small amount of clay before reaching a steady level near the detection limit (Figure 2a). The results of a ΔH_2Asc experiment show that reduction produced spikes of clay release and that the ensuing low I flush released a large pulse of clay before approaching the clay release detection limit (Figure 2b). In contrast, a high I flush following reduction produced a decline of turbidity to prereduction levels in only about 5 pore volumes (Figure 2c). The accompanying release of total Fe increased with

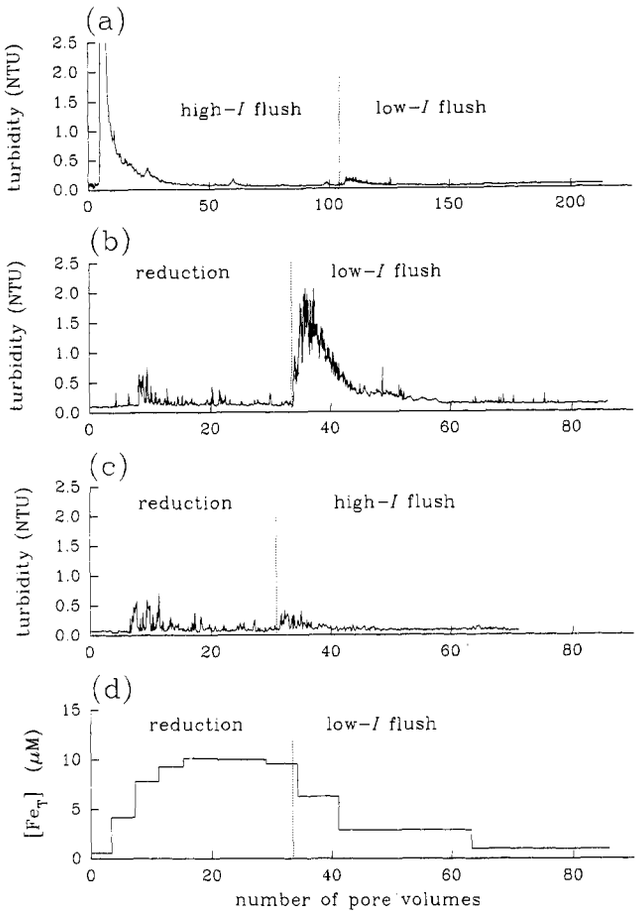

Figure 2. Raw data collected for column preflushing (sudden ΔI) and ascorbate reduction (ΔH_2Asc) experiments. Clay concentration was measured continuously; Fe was measured in integrated samples. (a) Example of the high I/low I flush at pH 4.8 used as preparation for further experiments. In initial flush, clay concentrations reached 28 NTU (off-scale peak) as clays loosened by column packing were removed. (b) Example of ascorbic acid/low I flush for 10^{-2} M H_2Asc_T and 5 × 10^{-4}M HAc/Ac^- at pH 4.8. Each reduction/low I flush was preceded by a high I/low I flush similar to that shown in panel a. During the low I flush, most of the clay was released in the first 5 pore volumes. (c) Example of ascorbic acid/high I flush for 10^{-2} M H_2Asc_T and 5 × 10^{-4} M HAc/Ac^- at pH 4.8. Very little turbidity was removed by the high I flush following reduction. (d) Example of ascorbic acid/low I flush for 10^{-2} M H_2Asc_T and 5 × 10^{-4} M HAc/Ac^- at pH 4.8. Fe release rate quickly increased to a plateau during reduction and slowly decreased during the flush.

H_2Asc addition and decreased gradually during the low I flush (Figure 2d).

In a preliminary test, we measured the long-term release of clay and Fe from the sediment. H_2Asc solution at 10^{-3} M was pumped through a column at pH 4.8 for 950 pore volumes. The release of clay and Fe were steady over the entire run. A total of only 0.5% of the total clay and 2.0% of the free Fe in the sediment was removed during this test.

In the "sudden" ΔI experiment (the high I/low I column flushing procedure), no significant difference between the time-averaged high I and low I clay release rate was discerned (Figure 3). In the "gradual" ΔI experiment, the clay release rate nearly doubled as I was decreased; however, the rate increase is probably not significant given the large error in measuring these low clay release rates. The total Fe release rates remained constant. Colloid

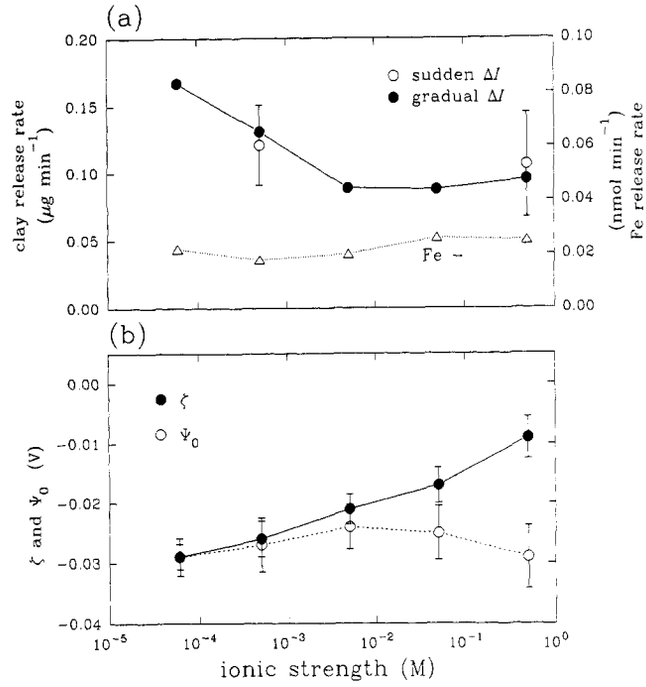

Figure 3. Effect of changing I on clay release rate. (a) A plot of clay release rates and Fe release rates vs ionic strength ([$NaNO_3$]) at pH 4.8. The effects of sudden ΔI from 0.5 to 0.0005 M (error bars represent $\pm 1\sigma$, $n = 22$ runs) and gradual ΔI over 4 orders of magnitude are shown. (b) Colloid ζ and surface potentials vs ionic strength (error bars $\pm 1\sigma$, $n = 20$ for all ζ-potential determinations).

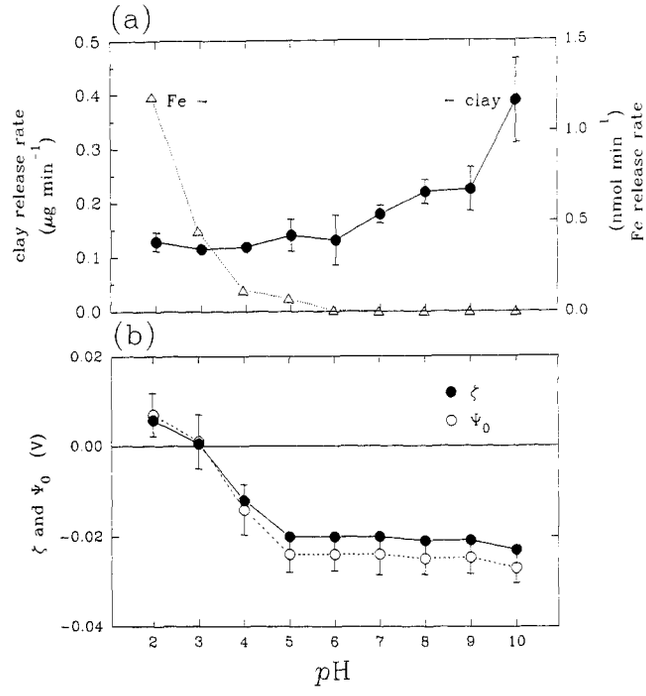

Figure 4. Effect of changing pH on clay release rate. (a) A plot of clay release rates and Fe release rates vs influent pH at $I = 1.0 \times 10^{-2}$ M $NaNO_3$. Data are average clay release rates for two runs. (b) Colloid ζ and surface potentials vs pH.

ζ-potentials became more negative with decreasing I, but surface potentials obtained with eq 2 did not vary much.

In the ΔpH experiments (Figure 4), the release rate tripled as pH increased, but most of increase occurred at pH > 7. The total Fe release rate decreased to below the detection limit at pH > 6. Colloid ζ-potentials reversed sign at approximately pH 3.0.

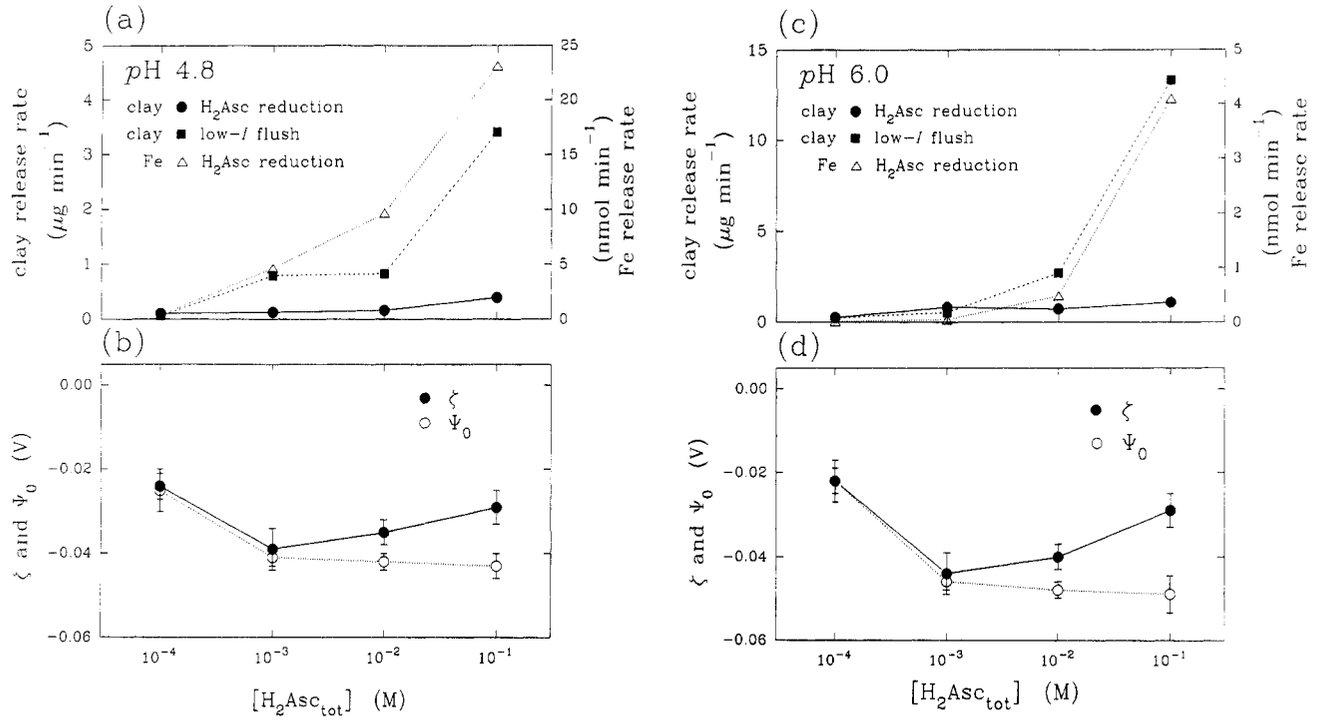

Figure 5. Effect of changing ascorbate concentration on clay release rate at pH 4.8 and 6.0. (a and c) Plots of clay release rates and Fe release rates vs ascorbic acid concentration at pH 4.8 (a) and 6.0 (c). (b and d) Colloid ζ and surface potentials vs ascorbic acid concentration at pH 4.8 (b) and 6.0 (d).

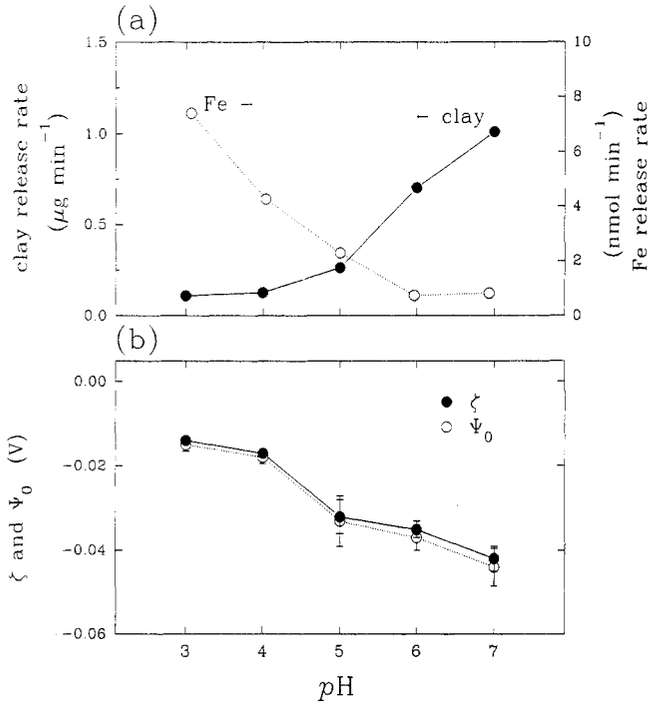

Figure 6. Effect of changing pH on clay release rate in the presence of 1.0×10^{-3} M H_2Asc_T. (a) Plot of clay release rates and Fe release rates vs pH. (b) Colloid ζ and surface potentials vs pH.

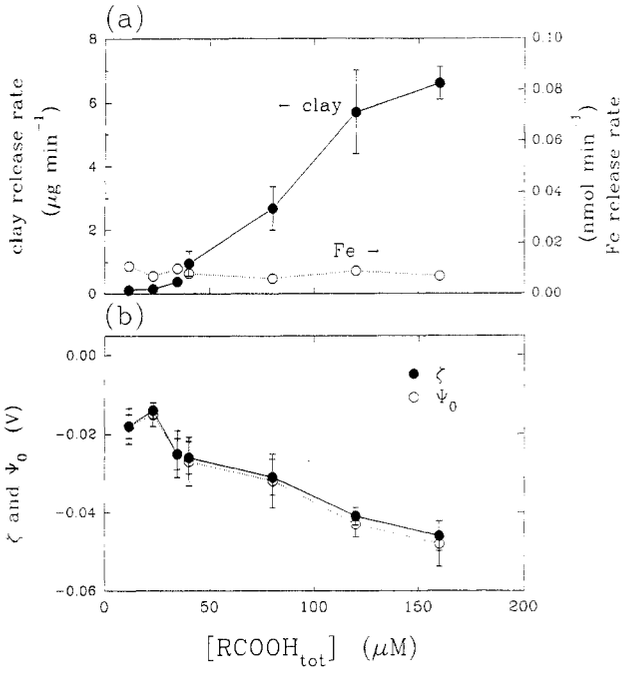

Figure 7. Effect of changing dodecanoic acid concentration on clay release rate. (a) Plot of clay release rates and Fe release rates vs dodecanoic acid concentration. (b) Colloid ζ and surface potentials vs dodecanoic acid concentration.

In the ΔH_2Asc experiments, Fe release rates clearly responded to the increase in $[H_2Asc_T]$, but the clay release rate increase was small (Figure 5). Colloid ζ-potentials reached a minimum at 10^{-3} M H_2Asc_T at both pH 4.8 and 6.0, but the estimated surface potentials became increasingly more negative with increasing $[H_2Asc_T]$. The time-averaged clay release rates during the low I flushes correlated well with the Fe release rates measured during reduction. When pH was varied at constant ascorbic acid concentration (ΔpH H_2Asc), clay release rates increased with increasing pH while the Fe release rates decreased (Figure 6). The colloid ζ-potentials and surface potentials became more negative with increasing pH.

In the presence of dodecanoic acid (ΔRCOOH), clay release rates increased dramatically, but the Fe release rate was low and constant (Figure 7). Colloid ζ-potentials became more negative with increasing dodecanoic acid concentration. When pH was increased in the presence of dodecanoic acid (ΔpH RCOOH), clay release rates

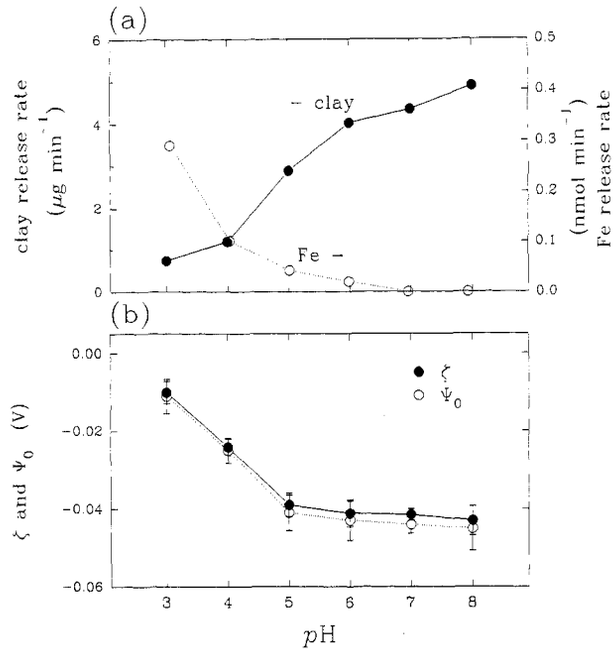

Figure 8. Effect of pH on clay release rate in the presence of 80 μM dodecanoic acid concentration. (a) Plot of clay release rates and Fe release rates vs pH. (b) Colloid ζ and surface potentials vs pH.

Table 3. Summary of Relationship between Clay Release Rate and Detachment Energy[a]

experiment	slope	$\phi^{det}/kT = 0$ intercept	R^2
ΔI	$-1.6 \pm 0.5 \times 10^{-3}$	-7.1 ± 0.1	0.73
ΔpH	$1.2 \pm 0.5 \times 10^{-3}$	-6.7 ± 0.1	0.42
ΔH_2Asc pH 4.8	$2.2 \pm 0.8 \times 10^{-3}$	-6.7 ± 0.1	0.91
ΔH_2Asc pH 6.0	$2.1 \pm 0.8 \times 10^{-3}$	-6.2 ± 0.1	0.76
ΔpH H_2Asc	$5.1 \pm 0.7 \times 10^{-3}$	-6.0 ± 0.3	0.94
ΔRCOOH	$6.2 \pm 2.7 \times 10^{-3}$	-5.4 ± 0.4	0.90
ΔpH RCOOH	$4.5 \pm 0.3 \times 10^{-3}$	-5.2 ± 0.3	0.98

[a] Slopes are calculated for the relationship log (clay release rate) vs ϕ^{det}/kT.

increased and the colloid ζ-potentials and surface potentials became more negative (Figure 8).

Natural Groundwater. The natural groundwater produced a relatively high mean clay release rate($2.3 \pm 0.4 \times 10^{-6}$ g min^{-1}, $n = 3$), but the mean Fe release rate was quite low ($8.1 \pm 7.1 \times 10^{-10}$ mol min^{-1}). The mean colloid ζ-potential was −30 mV, resulting in a ψ_0 of −32 mV. In low I flushes following the two shorter natural groundwater runs, turbidity decreased to levels measured in the preceding low I flush in less than 5 pore volumes.

Clay Release Rate—Detachment Energy Relationships. We assumed that interactions leading to colloid release were controlled by colloid–colloid and not colloid–grain interactions; therefore, we calculated the detachment energies using the surface potentials estimated from measured ζ values via eq 2. We surmise that these surface potentials, derived from experimentally determined electrophoretic mobilities, provide the best means for integrating the effects of most of the complicated effects that cannot be easily accounted for in estimating DLVO interactions in natural systems. The ζ correction accomplished by eq 2 appears to have removed the effect of high ionic strength and surface charge on ζ measurements.

For most of the experiments, clay release rates were positively correlated with ϕ^{det} (Table 3), with the notable exception of the ΔI experiment. For ΔI, clay release rates were negatively correlated with ϕ^{det}.

Discussion

Accuracy of Estimated Surface Potentials. The surface potentials estimated with the empirical ζ–ψ_0 relationship (eq 2) more accurately described the effects of solution chemistry on the colloid surfaces than did the ζ-potentials. For example, adsorption of ascorbate initially made ζ more negative; but at higher [$HAsc^-$], ζ became less negative because the ionic strength increased as well. The estimated surface potentials increased with [$HAsc^-$], consistent with the expected adsorption behavior and the colloid release behavior.

The estimated surface potentials may still inadequately represent the true surface potentials of the clay colloids. First, Smoluchowski's ζ–U relationship does not account for nonspherical colloids. The electrophoretic force is opposed by a fluid drag force, which, for an oblate ellipsoid with a major axis ratio of $b/a = 10$, is about 1.45 times greater than that of a sphere of the same radius (*40*). Thus, ζ of a clay particle with the same electrophoretic mobility as a spherical colloid should be about 50% greater than the ζ-potential of the spherical colloid. Second, ζ of the effluent colloids may have been substantially different from those of the colloids still attached. To achieve colloid concentrations high enough to measure ζ, we had to slightly agitate the column in duplicate experiments. Thus, we may have been measuring ζ of colloids whose detachment was aided by some motion greater than that of diffusion. Third, clay minerals possess permanent negative charge on their siloxane faces and amphoteric oxide functional groups on their edges and gibbsite faces. The clay surfaces may be partially coated by organic matter and other ions. The potentials of the faces and edges were measured as one overall ζ that would not describe colloid detachment behavior if, for example, the clay edges alone controlled the attachment of the colloids to the coatings. Conversely, this ability to measure overall ζ may also be considered an advantage in attempting to characterize the potentials of these heterogeneous surfaces.

Factors Controlling Colloid Detachment. Clay release rates were positively correlated with the detachment energy and unrelated to Fe release rates for most of the experiments (ΔpH, ΔpH H_2Asc, ΔRCOOH, and ΔpH RCOOH experiments). For these changes in solution chemistry, the forces controlling colloid detachment are clearly the electrostatic forces described by the DLVO theory. The agreement between the trends in the clay release rate and the detachment energies only indicates that DLVO forces appear to control clay release; it does not imply that the release mechanism is the same as that presented for model systems (*21*, *22*).

It is interesting to note that colloid mobilization is most often attributed to a decrease in ionic strength (*9–11*). The results of the ΔI experiment demonstrated that, in the presence of colloid phases of opposite charge (kaolinite and goethite at pH 4.8), the decrease in ionic strength did not cause a significant increase in the clay release rate. We surmise that the strong interaction between oppositely charged kaolinite and goethite mitigated the effect of ionic strength on the double-layer force between the colloids. Our understanding of the interactions between goethite and kaolinite is confirmed by the results of the ΔpH

experiment—the clay release rate does not significantly increase until the pH is raised to 7.0, just below the pH_{iep} of pure goethite (8.1–9.7; ref 41). The presence of adsorbed natural organic matter in the original sediment, 0.45 wt %, has perhaps shifted the isoelectric point of the goethite to a slightly lower pH, resulting in kaolinite mobilization at pH less than the pH_{iep}.

In the ΔI experiment, the clay release rate increased slightly as ionic strength decreased (although the increase in clay release rate was not significant), yet the calculated increase in detachment energy with decreasing ionic strength resulting in the only negative correlation between release rate and detachment energy. This result led us to explore the effects of ionic strength on colloid detachment in a system of hematite colloids and quartz grains (*26*). We found that an increase in x_{min} produced potential energy profiles without energy barriers in agreement with the experimental results. However, a similar approach did not yield agreement between the calculated detachment energies and the observed clay release rates here.

Effect of Reductive Dissolution on Clay Mobilization. The dissolution of iron(III) oxides have some influence on the clay release rate, as a comparison of the ΔpH and ΔpH H_2Asc experiments (Figures 4 and 6) shows—reduction accelerated the clay release rate, particularly at higher values of pH. This trend is reflected in the higher slope and intercept values of the clay release rate–ϕ^{det} relationship for the ΔpH H_2Asc data (Table 3). We surmise that the dissolution of iron(III) oxides enhanced the clay release rate by changing the colloid–colloid interaction from kaolinite–goethite–kaolinite to the more repulsive kaolinite–kaolinite. We were not able to observe this change directly because we measured ζ of only the released colloids.

The experiments in which $[H_2Asc_T]$ was varied and followed by a low I flush further illustrated the effect of dissolution of the goethite cement (Figure 5). The lowest concentration of H_2Asc_T (10^{-4} M) had little effect on the clay release rate relative to the rate measured at the same pH without H_2Asc present. At 10^{-3} M H_2Asc_T, iron(III) oxides were dissolved more rapidly, and the clay release rate tripled at pH 6 and increased slightly at pH 4.8. At the two higher H_2Asc_T concentrations, the rate of iron(III) oxide dissolution kept increasing, but the clay release rates began to level off. We surmise that the clay release rate reached a plateau as the Fe release rate continued to rise because of the counteracting effect of increasing I. The increase in I decreased the repulsive force between the clay colloids even though the dissolution of iron(III) oxides may have changed the colloid–colloid interactions from kaolinite–goethite–kaolinite to kaolinite–kaolinite.

When the high I H_2Asc solution was replaced by the low I flush solution, the colloids that had been "loosened" by goethite dissolution, but not released, were rapidly flushed. In the low I flushes, the rates and total amounts of clay and Fe release were directly related. The same effect was not observed for the natural groundwater, suggesting that the natural organic matter did not cause substantial reductive dissolution of the goethite.

Surfactant Adsorption and Clay Release. Dodecanoic acid was added at concentrations of 0.06–0.8 μg of C L^{-1}, far less than the ~1.0 mg of C L^{-1} found in the oxic groundwater nearby (*14*). However, in terms of ionizable carboxylate groups, the addition of dodecanoic acid represented much higher concentrations of organic matter than the groundwater NOM. At pH 4.8, the dodecanoate concentration ranged from about 10 to 140 μequiv L^{-1}. In Pine Barrens groundwater, NOM consists mainly of humic substances (*42*). Terrestrial humic substances typically contain about 5 mequiv g^{-1} carboxyl groups ($pK_a \approx 4.0$) (*43*), resulting in about 4.3 mequiv g^{-1} of ionized functional groups at pH 4.8. Thus, the 1.0 mg of C L^{-1} of NOM in the natural groundwater with which the natural groundwater had been equilibrated contains only about 4.3 μequiv L^{-1} of ionized carboxyl groups.

The adsorption of dodecanoate in the range of [RCOOH] used in these experiments is capable of reversing the surface charge of hematite at pH 5.2 (*44*). Although we were not able to directly observe the effect of dodecanoate adsorption onto positively charged oxides, we surmise that dodecanoate adsorption reversed the surface charge of goethite and the positively charged oxide sites on the clay edges, resulting in strongly repulsive interactions and rapid colloid release. The dramatic effect of dodecanoic acid addition suggests that, even in the presence of the 0.45 wt % of organic matter measured in the sediment, positively charged sites remained to adsorb dodecanoate.

Dodecanoate adsorption, which is primarily physical (ion exchange, hydrophobic interactions) but may include some specific ligand exchange, particularly with iron(III) oxides (*45, 46*), probably resulted in hemimicelle formation. Hemimicelle formation usually occurs at about 10^{-3}–10^{-2} of the critical micelle concentration (CMC) of a surfactant (*47, 48*). The CMC of sodium dodecanoate is 24 mM (*49*); thus, we expect hemimicelle formation at about 24–240 μM dodecanoate. This corresponds well with the [$RCOO^-$] concentration at which the clay release rate began to increase rapidly, about 16–48 μM $RCOO^-$.

Natural Groundwater and Clay Release. The relatively high clay release rate caused by the natural groundwater accompanied by low Fe release rate suggests that the natural groundwater affected clay release in the same manner as dodecanoic acid. The mechanisms of natural organic matter (NOM) adsorption to mineral surfaces may include both ligand exchange (*50–52*), ion exchange, and hydrophobic interactions (*53, 54*). Recently, the adsorption of surfactants has been modeled accounting for both mechanisms (*44, 55*).

If ion exchange and hemimicelle formation are the dominant mechanisms of both NOM and dodecanoate adsorption, then we would expect that comparable amounts NOM and dodecanoate (in terms of ionized functional groups) would cause similar clay release rates. At pH 4.2, the 20 mg of C L^{-1} of NOM in the natural groundwater may contain about 62 μequiv L^{-1} of carboxylate groups. The natural groundwater released clay at about the same rate as 80 μM dodecanoic acid (33 μM $RCOO^-$) solution at pH 4.8, suggesting that their adsorption mechanisms may be similar.

Implications for Colloid Mobilization. Based on the clay release rate of 1.5×10^{-7} g min^{-1} measured at pH 4.8 and low ionic strength, hydraulic gradients as high as 0.17 (*56*), hydraulic conductivity as high as 10^{-6} m s^{-1}, and porosity of 0.44 (*30*), flushing the clay from the 6-m deep column of sand that has been decemented below the swamp (*16*) would require about 75 000 yr without an effective colloid-mobilizing agent. This time is considerably longer than the ca. 10 000 yr that the existing swamp terrain is presumed to have been present at this site following glaciation. However, at the clay release rate of 2.3×10^{-6}

g min^{-1} measured in the presence of NOM in the natural groundwater, the clay from the decemented column of sand could be removed in only 4900 yr.

Dissolution of the free Fe in that sediment would require 13 500 yr at the Fe release rate of 8.1×10^{-10} mol min^{-1} measured in the presence of the natural groundwater. If all the clay released is kaolinite, the clay release rate could be expressed as 8.9×10^{-9} mol min^{-1}. About 11 mol of kaolinite is released for every mole of goethite dissolved, while the molar ratio of kaolinite/goethite ≈ 5 in the coatings. The accelerated release of kaolinite suggests that goethite colloids must be mobilized prior to dissolution. These release rates may explain our observation of both kaolinite and goethite colloids in the natural groundwater (*14*); however, we did not observe ferric oxyhydroxide colloids in the column effluent.

Contaminant plumes emanating from waste sites are typically near neutral pH, anoxic, high in ionic strength, and capable of dissolving reducible oxides from the sediments (*57, 58*). While iron(III) oxide dissolution may occur, high ionic strength may inhibit the release of colloids. Contaminant plumes also contain surfactant-like compounds (*59*) that may cause colloid mobilization. Surfactants containing phosphate and sulfonate functional groups, which form strong specific surface complexes with most oxides, may be even more effective than carboxylic acids at reversing the surface charge of cementing phases and mobilizing colloids.

Conclusions

Colloids can be mobilized from a natural sediment primarily by increasing the electrostatic repulsion between the colloid surfaces. Iron(III) oxide reductive dissolution was not necessary to mobilize clay colloids, although decementation did accelerate clay release rates under some conditions, possibly by changing colloid–grain interactions from kaolinite–goethite–kaolinite to the more repulsive kaolinite–kaolinite. A decrease in ionic strength caused an insignificant increase in the clay release rate, indicating that changing ionic strength did not promote clay release in the presence of oppositely charged kaolinite and goethite colloids. The results of these experiments suggest that, in typical landfill leachates, surfactants may present the most effective means of generating colloids capable of facilitating contaminant transport.

Acknowledgments

The authors are grateful to Harry Hemond, John MacFarlane, Jonathan Clapp, and Martha Russo for help with sample collection; to John MacFarlane for graphics; to Harry Hemond, François Morel, and two anonymous reviewers for insightful comments on the manuscript; and to Dr. Frank Wobber and the Subsurface Science Program of the Department of Energy for continued support under Contracts DE-FG02-86ER60413 and DE-FG02-89ER60846. Portions of this work were first presented at the Fall Meeting of the American Geophysical Union in December 1992.

Abbreviations and Symbols

ϵ	dielectric constant of water
ϵ_0	permittivity of free space
ζ	zeta potential
η	viscosity of water
κ	Debye–Hückel parameter
ϕ^{det}	intersurface potential energy barrier associated with detachment
ϕ^{dl}	double-layer intersurface potential energy
ϕ_{max}	primary maximum in intersurface potential energy
ϕ_{min1}	primary minimum in intersurface potential energy
ϕ^{tot}	total intersurface potential energy
ψ_0	surface potential
ψ_{scdl}	surface potential calculated by surface complexation/double-layer model
ϕ^{vdw}	van der Waals intersurface potential energy
B	baseline turbidity measurement
BET	Brunauer–Emmett–Teller
DLVO	Derjaguin–Landau–Verway–Overbeek
EDX	energy-dispersive X-ray spectroscopy
GF-AAS	graphite furnace-atomic absorption spectrophotometer
H_2Asc, $Hasc^-$	ascorbic acid, ascorbate ion
HAc, Ac^-	acetic acid, acetate ion
HPLC	high-performance liquid chromatography
I	ionic strength
k	Boltzmann constant
pH_{iep}	isoelectric point
PTFE	polytetrafluoroethylene
RCOOH, $RCOO^-$	dodecanoic acid, dodecanoate
SEM	scanning electron microscopy
T	absolute temperature
T_{NTU}	turbidity
TPTZ	2,4,6-tri(2-pyridyl)-1,3,5-triazine
U	electrophoretic mobility
x_{min}	distance of closest approach of colloid to grain
$[K]$	kaolinite suspension concentration

Literature Cited

(1) Buddemeier, R. W.; Hunt, J. R. *Appl. Geochem.* **1988**, *3*, 535–548.
(2) McCarthy, J. F.; Zachara, J. M. *Environ. Sci. Technol.* **1989**, *23*, 496–502.
(3) Penrose, W. R.; Polzer, W. L.; Essington, E. H.; Nelson, D. M.; Orlandini, K. A. *Environ. Sci. Technol.* **1990**, *24*, 228–234.
(4) Magaritz, M.; Amiel, A. J.; Ronen, D.; Wells, M. C. *J. Contam. Hydrol.* **1990**, *5*, 333–347.
(5) Langmuir, D. Geochemistry of iron in a coastal-plain groundwater of the Camden, New Jersey area. *U.S. Geol. Surv. Prof. Pap.* **1969**, *No. 650–C*, C224-C235.
(6) Gschwend, P. M.; Reynolds, M. D. *J. Contam. Hydrol.* **1987**, *1*, 309–327.
(7) Degueldre, C.; Baeyens, B.; Goerlich, W.; Riga, J.; Verbist, J.; Stadelmann, P. *Geochim. Cosmochim. Acta* **1989**, *53*, 603–610.
(8) Kaplan, D. I.; Bertsch, P. M.; Adriano, D. C.; Miller, W. P. *Environ. Sci. Technol.* **1993**, *27*, 1193–1200.
(9) Nightingale, H. I.; Bianchi, W. C. *Ground Water* **1977**, *15*, 146–152.
(10) Khilar, K. C.; Fogler, H. S. *J. Colloid Interface Sci.* **1984**, *101*, 214–224.
(11) McDowell-Boyer, L. M. *Environ. Sci. Technol.* **1992**, *26*, 586–593.
(12) Harris, W. G.; Carlisle, V. W.; Chesser, S. L. *Soil Sci. Am. J.* **1987**, *51*, 1673–1677.
(13) Gschwend, P. M.; Backhus, D. A.; MacFarlane, J. K.; Page, A. L. *J. Contam. Hydrol.* **1990**, *6*, 307–320.
(14) Ryan, J. N.; Gschwend, P. M. *Water Resour. Res.* **1990**, *26*, 307–322.

(15) Ronen, D.; Margaritz, M.; Weber, U.; Amiel, A. J.; Klein, E. *Water Resour. Res.* **1992**, *28*, 1279–1291.
(16) Ryan, J. N.; Gschwend, P. M. *Geochim. Cosmochim. Acta* **1992**, *56*, 1507–1521.
(17) Derjaguin, B. V.; Landau, L. D. *Acta Physicochim. SSSR* **1941**, *14*, 633.
(18) Verwey, E. J. W.; Overbeek, J.Th.G. *Theory of the Stability of Lyophobic Colloids*; Elsevier: Amsterdam; 1948.
(19) Kia, S. F.; Fogler, H. S.; Reed, M. G. *J. Colloid Interface Sci.* **1987**, *118*, 158–168.
(20) Cerda, C. *Colloids Surf.* **1987**, *27*, 219–241.
(21) Dahneke, B. *J. Colloid Interface Sci.* **1975**, *50*, 89–107
(22) Ruckenstein, E.; Prieve, D. C. *Am. Inst. Chem. Eng. J.* **1976**, *22*, 276–283.
(23) Kallay, N.; Barouch, E.; Matijević, E. *Adv. Colloid Interface Sci.* **1987**, *27*, 1–42.
(24) Barouch, E.; Matijević, E.; Wright, T. H. *Chem. Eng. Commun.* **1987**, *27*, 29–40.
(25) Vaidya, R. N.; Fogler, H. S. *Colloids Surf.* **1990**, *50*, 215–229.
(26) Ryan, J. N.; Gschwend, P. M. *J. Colloid Interface Sci.* **1994**, *164*, 21–34.
(27) Ryan, J. N. Clay Colloid Mobilization in an Iron Oxide-Coated Sand. Ph.D. Dissertation, Massachusetts Institute of Technology, 1992.
(28) Ryan, J. N. Gschwend, P. M. *Clays Clay Miner.* **1991**, *39*, 509–518.
(29) Sugimura, Y.; Suzuki, Y. *Mar. Chem.* **1988**, *24*, 105–131.
(30) Rhodehamel, E. C. In *Pine Barrens: Ecosystem and Landscape*; Forman, R. T. T., Ed.; Academic Press: New York, 1979; pp 39–60.
(31) Dougan, W. K.; Wilson, A. L. *Water Treat. Exam.* **1973**, *22*, 100–113.
(32) Hunter, R. J. *Zeta Potential in Colloid Science*; Academic Press: New York, 1981.
(33) Hamaker, H. C. *Physica* **1937**, *4*, 1058–1072.
(34) Hogg, R.; Healy, T. W.; Fuerstenau, D. W. *Trans. Faraday Soc.* **1966**, *62*, 1638–1651.
(35) Overbeek, J. Th. G. In *Colloid Science*; Kruyt, H. R., Ed.; Elsevier: Amsterdam, 1952; p 245.
(36) Wiese, G. R.; Healy, T. W. *J. Colloid Interface Sci.* **1975**, *51*, 427–433.
(37) Dzombak, D. A.; Morel, F. M. M. *Surface Complex Modeling. Hydrous Ferric Oxide*; Wiley-Interscience: New York, 1990.
(38) Westall, J. C.; Zachary, J. L.; Morel, F. M. M. *MINEQL—A computer program for the calculation of chemical equilibrium composition of aqueous systems*; Technical Note 18; R. M. Parsons Laboratory, Massachusetts Institute of Technology: Cambridge, 1976.
(39) Parks, G. A. In *Equilibrium Concepts in Natural Water Systems*; Stumm, W., Ed.; American Chemical Society Advances in Chemistry Series 67; ACS: Washington, DC, 1967; pp 121–160.
(40) Hiemenz, P. C. *Principles of Colloid and Surface Chemistry*, 2nd ed.; Marcel Dekker: New York, 1986; p 88.
(41) Zeltner, W. A.; Anderson, M. A. *Langmuir* **1988**, *4*, 469–474.
(42) Crerar, D. A.; Means, J. L.; Yuretich, R. F.; Borcsik, M. P.; Amster, J. L.; Hastings, D. W.; Knox, G. W.; Lyon, K. E.; Quiett, R. F. *Chem. Geol.* **1981**, *33*, 23–44.
(43) Thurman, E. M. *Organic Geochemistry of Natural Waters*; Nijhoff/Junk: Dordrecht, 1985.
(44) Liang, L.; Morgan, J. J. In *Chemical Modeling of Aqueous Systems II*; Melchoir, D. C., Bassett, R. L., Eds.; American Chemical Society Symposium Series 416; ACS: Washington, DC, 1990; pp 293–308.
(45) Peck, A. S.; Raby, L. H.; Wadsworth, M. E. *Trans. Metall. Soc. AIME* **1966**, *235*, 301–307.
(46) Han, K. N.; Healy, T. W.; Fuerstenau, D. W. *J. Colloid Interface Sci.* **1971**, *44*, 407–414.
(47) Fuerstenau, D. W. *J. Phys. Chem.* **1956**, *60*, 981–985.
(48) Somasundaran, P.; Healy, T. W.; Fuerstenau, D. W. *J. Phys. Chem.* **1964**, *68*, 3562–3566.
(49) Lichtenberg, D.; Robson, R. J.; Dennis, E. A. *Biochim. Biophys. Acta* **1983**, *737*, 285–304.
(50) Davis, J. A. *Geochim. Cosmochim. Acta* **1982**, *46*, 2381–2393.
(51) McKnight, D. M.; Bencala, K. E.; Zellweger, G. W.; Aiken, G. R.; Feder, G. L.; Thorn, K. A. *Environ. Sci. Technol.* **1992**, *26*, 1388–1396.
(52) Gu, B.; Schmitt, J.; Chen, Z.; Liang, L.; McCarthy, J. F. *Environ. Sci. Technol.* **1994**, *28*, 38–46.
(53) Jardine, P. M.; Weber, N. L.; McCarthy, J. F. *Soil Sci. Soc. Am. J.* **1989**, *53*, 1378–1385.
(54) Ochs, M.; Ćosović, B.; Stumm, W. *Geochim. Cosmochim. Acta* **1994**, *58*, 639–650.
(55) Rea, R. L.; Parks, G. A. In *Chemical Modeling of Aqueous Systems II*; Melchoir, D. C., Bassett, R. L., Eds.; American Chemical Society Symposium Series 416; ACS: Washington, DC, 1990; pp 260–271.
(56) Lord, D. G.; Barringer, J. L.; Johnsson, P. A.; Schuster, P. F.; Walker, R. L.; Fairchild, J. E.; Sroka, B. N.; Jacobsen, E. Hydrogeochemical data from an acidic deposition study at McDonalds Branch basin in the New Jersey Pinelands, 1983–1986. *U.S. Geol. Surv. Open-File Rep.* **1990**, *No. 88-500*.
(57) Kimmel, G. E.; Braids, O. C. Leachate plumes in ground water from Babylon and Islip landfills, Long Island, New York. *U.S. Geol. Surv. Prof. Pap.* **1980**, *No. 1085*.
(58) Nicholson, R. V.; Cherry, J. A.; Reardon, E. J. *J. Hydrol.* **1983**, *63*, 131–176.
(59) Thurman, E. M.; Barber, L. B., Jr.; LeBlanc, D. *J. Contam. Hydrol.* **1986**, *1*, 143–161.

Received for review January 4, 1994. Revised manuscript received May 19, 1994. Accepted May 23, 1994.[⊛]

[⊛] Abstract published in *Advance ACS Abstracts,* July 1, 1994.